

Photoemissive, Photoconductive, and Optical Absorption Studies of Alkali-Antimony Compounds

W. E. SPICER

RCA Laboratories, Princeton, New Jersey

(Received May 29, 1958)

By means of absorption and photoconductivity measurements, the following band gaps were found: Na_3Sb —1.1 eV; K_3Sb —1.1 eV; Rb_3Sb —1.0 eV; Cs_3Sb —1.6 eV; and $(\text{NaK})_3\text{Sb}$ —1.0 eV. A model has been derived for the photoemission from these materials which fits the three last materials listed above in addition to the $(\text{NaK})_3\text{Sb}$ with surface layers of Cs or Rb added. The electron affinities found from the photoemissive data using this model were as follows: Rb_3Sb —1.2 eV; Cs_3Sb —0.45 eV; $(\text{NaK})_3\text{Sb}$ —1.0 eV; $[\text{Rb}](\text{NaK})_3\text{Sb}$ —0.70 eV; and $[\text{Cs}](\text{NaK})_3\text{Sb}$ —0.55 eV. The electron affinity of K_3Sb was estimated to be between 1.1 and 1.8 eV and that of Na_3Sb to be between 2.0 and 2.4 eV. By means of the temperature dependence of the photoemission, Rb_3Sb , Cs_3Sb , and the multi-alkali materials were found to have p -type conductivity; whereas K_3Sb and Na_3Sb were found to have n -type conductivity.

I. INTRODUCTION

ALKALI metals react with antimony to form semiconducting compounds of the general formula $M_3\text{Sb}$, where M represents one or more alkali metals.^{1,2} These alkali antimonides are of particular interest because they include the most efficient photoemitters known, e.g., Cs_3Sb and $[\text{Cs}](\text{NaK})_3\text{Sb}$. In order to obtain an understanding of this photoemissive process, absorption, photoconductive, and photoemissive studies have been made on these materials and values obtained for their band gaps and electron affinities. In addition, a theoretical model has been derived for the photoemission from these materials. The materials studied were: Na_3Sb , K_3Sb , Rb_3Sb , Cs_3Sb , and the multi-alkali³ compounds $(\text{NaK})_3\text{Sb}$, $[\text{Cs}](\text{NaK})_3\text{Sb}$, and $[\text{Rb}](\text{NaK})_3\text{Sb}$. Here $[\text{Cs}]$ or $[\text{Rb}]$ placed before $(\text{NaK})_3\text{Sb}$ indicates a surface layer of Cs or Rb.

Although there is little literature concerning the electrical and optical properties of the other materials studied here, Cs_3Sb has been investigated quite extensively. Burton,⁴ Morgulis *et al.*,⁵ and Wallis,⁶ as well as others, have measured the absorption of such films. Their results are shown in curves (1) and (2) of Fig. 1.

Burton⁴ has also established that the high photoemissive yield in Cs_3Sb is due to intrinsic photoemission, i.e., excitation of electrons from the valence band, and has reported that the photoelectrons come from a mean depth of about 250 Å in the material. There is a large variation in the spectral distribution of the photoemissive yield curves of Cs_3Sb as reported by different workers. For example, the curves of Apker and Taft⁷ rise much more gradually and tend to reach a

plateau at a higher energy than those of Burton⁴ or Harper and Choyke.^{8*} Since the formation of the gross 3:1 compound is relatively straightforward, it is probable that these differences are related to differences in the electronic escape probabilities and not to differences in the optical absorption in these materials.

Borzyak⁹ and Sakata¹⁰ have reported that Cs_3Sb shows p -type conduction. Borzyak has also found that by forcing an excess of Cs into the layer, the conductivity may be changed from p to n type. Thus excess alkali acts like a donor. Sommer¹¹ has extended the measurements of Borzyak and found that the conductivity of Cs_3Sb is increased by Sb addition; thus indicating that excess Sb produces acceptors. Sommer has also done similar experiments on the other materials studied here. He found that addition of the alkali constituent decreased the conductivity of the multi-alkalis; whereas it increased the conductivity of K_3Sb and Na_3Sb . Thus, it appears that the multi-alkalis are p type and Na_3Sb and K_3Sb are n type. Rb_3Sb usually exhibited n -type behavior (i.e., an increase in resistivity on Sb addition); however, since the maximum increase in resistance obtainable was less than for Na_3Sb or K_3Sb and, since on a few occasions the resistance decreased on Sb addition, the results were not as clear-cut as for the other materials.

II. EXPERIMENTAL METHODS

A. General Techniques

The experimental equipment was built around a model 12B Perkin-Elmer monochromator as described

⁸ W. J. Harper and W. J. Choyke, *Rev. Sci. Instr.* **27**, 966 (1956).

* *Note added in proof.*—Dr. Apker, Dr. Taft, and Dr. Philipp have made additional studies of Cs_3Sb and report, in a private communication, reasonable agreement with the curves of Burton, Harper, and Choyke, and those of this work. Therefore, this type of spectral response curve can be considered to be normal for Cs_3Sb . It should be mentioned that the velocity distributions reported by Apker and Taft⁷ have also been found by these workers in Cs_3Sb layers with the normal spectral response curves.

⁹ P. G. Borzyak, *Zhur. Tekh. Fiz. U.S.S.R.* **20**, 923 (1950); [*see Chem. Abstr.* **45**, 437 (1951)].

¹⁰ T. Sakata, *J. Phys. Soc. Japan* **8**, 125 (1953); **9**, 1030 (1954).

¹¹ A. H. Sommer, *J. Appl. Phys.* (to be published).

¹ A. H. Sommer, *Proc. Phys. Soc. (London)* **55**, 145 (1943).

² G. Brauer and E. Zintl, *Z. physik Chem.* **37B**, 323 (1937).

³ A. H. Sommer, *Rev. Sci. Instr.* **26**, 725 (1955).

⁴ J. A. Burton, *Phys. Rev.* **72**, 531(A) (1947). Burton's data are given by V. K. Zworykin and E. G. Ramberg, in *Photoelectricity* (John Wiley and Sons, Inc., New York, 1949), p. 59.

⁵ Morgulis, Borzyak, and Dyatlovitskaya, *Izvest. Akad. Nauk S.S.S.R.* **12**, 126 (1948).

⁶ G. Wallis, *Ann. Physik* **17**, 401 (1956).

⁷ L. Apker and E. Taft, *J. Opt. Soc. Am.* **43**, 78 (1953).

by DeVore.¹² Either a tungsten or a A-H-6 mercury lamp was used as a light source. When necessary, optical filters were used to eliminate scattered light. For the photoemission measurements, a monochromator slit width of 0.25 mm was used giving a band width at half maximum intensity of 0.025 ev or less. A slit width of between 0.25 and 0.5 mm was used for the photoconductivity and absorption measurements.

Films of the antimonides were produced by evaporating Sb onto the walls of the vacuum tube and reacting it to completion with the alkali metal vapor(s).¹³ The vacuum tubes were designed to allow for the measurement of photoconduction, photoemission, and optical absorption on the same surface. As the object of this work was to survey a number of materials without demanding extreme accuracy in the measurements, the design of the tube was kept as simple as possible. The tubes were usually cylindrical with two evaporated Al electrodes, 2 cm long, separated by a 2-mm gap, serving as cathode contacts. The antimony evaporator faced the slit and was used as an anode for the photoemission measurements. The tubes were of either Pyrex or quartz.

All the results presented, whether for absorption, photoconduction, or photoemission, are representative of those made on two or more tubes. The results were reproducible from tube to tube unless otherwise noted.

B. Optical Absorption

In making the absorption measurements, the experimental tube was positioned so that the intensity of the reflected light, I_R , and the intensity of the transmitted light, I , could be measured by moving the pickup cell without disturbing the tube or light beam. An Eastman Kodak "Ektron" PbS photoconductor was used as the pickup cell for the infrared and visible region and an RCA-1P28 photomultiplier was used for near ultraviolet.

Although some measure of the sample thickness could be obtained by measuring the transmission of the antimony film from which it was formed,¹⁴ it was felt that the thickness was not well enough known to justify the complicated analysis necessary for exact determination of the absorption coefficient and index of refraction. However, the reflection was measured, and, as a first approximation, the absorption data will be plotted as

$$1 - \left(\frac{I}{I_0} \frac{1}{1-R} \right),$$

where I_0 is the intensity of the incident light and R is I_R/I_0 . In this approximation, no correction is made for

¹² H. B. DeVore, RCA Rev. **13**, 453 (1952); H. B. DeVore and J. W. Dewdney, Phys. Rev. **83**, 805 (1951).

¹³ For details of the activation process see A. H. Sommer and W. E. Spicer, in *Methods of Experimental Physics*, edited by A. Lark-Horowitz [Academic Press, Inc., New York (to be published)], Vol. 6, Part B].

¹⁴ M. Rome, J. Appl. Phys. **26**, 166 (1955).

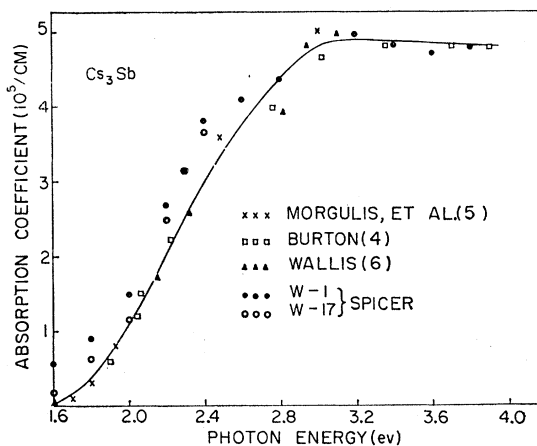


Fig. 1. Cs_3Sb absorption coefficients obtained by various workers. A coefficient of $10^6/\text{cm}$ at 3.0 ev was assumed in the present work.

the absorption which occurs in multiple reflections of the light, and thus absorption coefficients obtained from these data will tend to be high. Since other workers⁴⁻⁶ have measured the absorption coefficient of Cs_3Sb , a measure of the accuracy of the method may be obtained by a comparison of the results of this work to their results. This is done in Fig. 1. Since the thicknesses of our surfaces were not well known, these were obtained by taking a value of $5 \times 10^5/\text{cm}$ for the absorption coefficient at 3.0 ev. Data obtained from two of our surfaces are shown. In general, there is fairly good agreement with the published data; however, as is to be expected, our data tend to show higher absorption near the threshold.

Because of the extreme thinness of the samples, significant absorption measurements may be obtained for absorption coefficients between about 10^4 and $10^6/\text{cm}$ but not for smaller coefficients.¹⁵ Thus the fundamental absorption edge is not well defined by the absorption measurements. Fortunately, the fundamental edge is usually defined sufficiently well by the photoconductivity data.

C. Photoconductivity Measurements

For the photoconductivity measurements, between 1 and 22 volts were applied across the gap between the two electrodes. In these measurements, it was found that the photocurrent usually decreased to an asymptotic value after the voltage was applied. By reversing the voltage or removing it for 10 or 20 minutes, the original photoconductive value could be obtained. These effects are probably associated with electrolytic and diffusion transport near the electrode interface,^{16,17}

¹⁵ For other curves of absorption in the fundamental region see, for example, W. C. Dash and R. Newman, Phys. Rev. **99**, 1151 (1955); A. F. Gibson, Proc. Phys. Soc. (London) **B63**, 756 (1950).

¹⁶ H. Miyazawa and S. Fukuhara, J. Phys. Soc. Japan **1**, 645 (1952).

¹⁷ W. Widmaier and R. W. Engstrom, RCA Rev. **16**, 109 (1955).

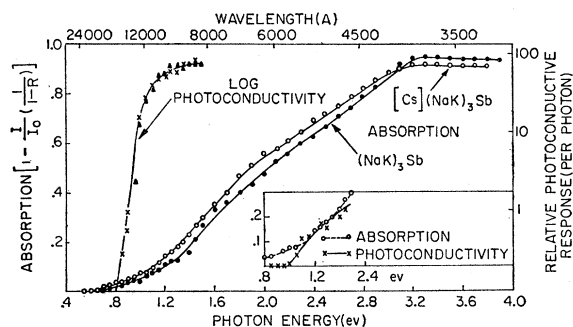


FIG. 2. Absorption and photoconductivity of $(\text{NaK})_3\text{Sb}$ and $[\text{Cs}](\text{NaK})_3\text{Sb}$. A band gap of 1.0 eV is obtained from these data.

but did not induce any measurable change in the photoemissive or absorption characteristics of the material. In making photoconductive measurements, the voltage was either left on long enough to approach the asymptotic photoconductive value or was reversed after each measurement and left on for a given amount of time before the next measurement. In order to remove any systematic errors which might have occurred despite these precautions, the data (photoconductivity *versus* photon energy) were taken in a random order of photon energy.

If external photoelectrons are created, these are attracted to the positive electrode and form a current which masks the internal photocurrent. This makes it impossible to extend the photoconductive measurements much beyond the photoemissive threshold.

III. ABSORPTION AND PHOTOCONDUCTIVITY RESULTS

The absorption and photoconductivity results are presented in Figs. 2 through 6 where the absorption and the logarithm of photoconductivity are plotted

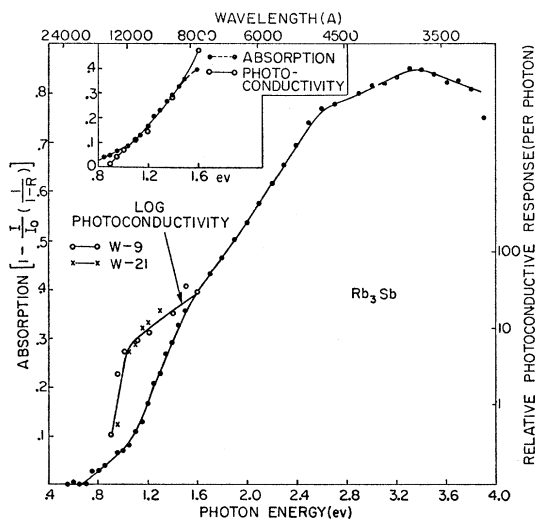


FIG. 3. Absorption and photoconductivity of Rb_3Sb . A band gap of 1.0 eV is obtained from these data.

versus photon energy. In order to indicate that the photoconductivity parallels the absorption fairly well for values of $h\nu$ above the photoconductive threshold, an insert is added giving linear plots of photoconductivity and absorption normalized at one point.

As can be seen in Figs. 2 through 5, the photoconductivity data were usually characterized by the sharp rise to be expected at the edge of fundamental absorption. The band gap will be taken as the value of photon energy at which the photoconductivity stops rising exponentially. As can be seen from the figures, the values so obtained agree with those which might be estimated from the absorption data. The resulting values of band gap are given in Table I of Sec. V.

Only for Cs_3Sb (Fig. 6) did the photoconductivity fail to show a sharp break on a semilog plot. This would seem to indicate that either impurity photoconductivity

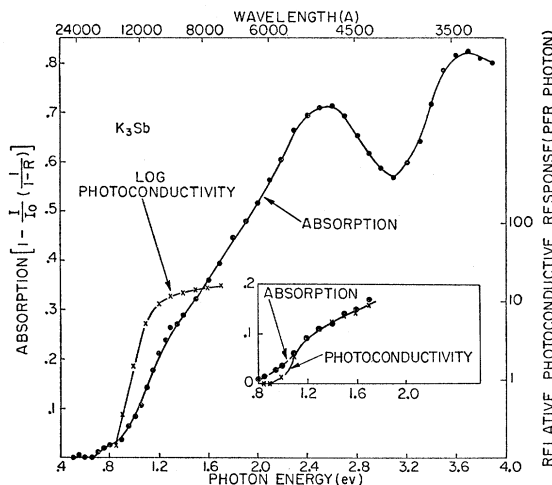


FIG. 4. Absorption and photoconductivity of K_3Sb . A band gap of 1.1 eV is obtained from these data. The absorption minimum at 3.1 eV was quite reproducible.

or an indirect optical absorption¹⁸ process is obscuring the absorption edge. In any case, the value of the band gap must be estimated from the absorption data. Here it is hard to arrive at a precise value since the thinness of the samples makes it difficult to obtain absorption coefficients of less than $10^4/\text{cm}$. However, Wallis⁶ and Eckart¹⁹ have fitted an equation of the form $\alpha = C(h\nu - E_G)^{3/2}$, where α is the absorption coefficient and C is a constant, to the experimental values of the absorption coefficients. Wallis obtains from his fit a value of 1.6 eV for the band gap energy E_G and Eckart a value of 1.7 eV. These values probably indicate an upper limit of the band gap energy.

¹⁸ The fact that the square root of the photoconductive response is linear in $h\nu$ would support the indirect optical absorption process (see insert Fig. 6) with a band gap of about 1.0 eV; however, this evidence is too isolated to take seriously unless it is confirmed by other evidence.

¹⁹ F. Eckart, *Ann. Physik* **19**, 133 (1956).

It was found that both the absorption and the photoconductivity curves of $(\text{NaK})_3\text{Sb}$ and $[\text{Cs}]-(\text{NaK})_3\text{Sb}$ were identical within experimental error (Fig. 2). This reaffirms Sommer's previous conclusion³ that the Cs added to $(\text{NaK})_3\text{Sb}$ only reduces the electron affinity and does not affect the bulk properties of the material.

The forms of the absorption curves are of general interest. In particular, the rate at which the absorption increases with $h\nu$ and the value of photon energy at which the absorption becomes relatively constant should be noted. The Cs_3Sb absorption (Fig. 6) had the largest rate of increase and began to level off at the smallest value of photon energy (about 2.4 eV) of any of the materials. Rb_3Sb began to level off at about 2.6 eV (Fig. 3) and Na_3Sb at about 2.8 eV (Fig. 5). K_3Sb showed strong structure in its absorption above

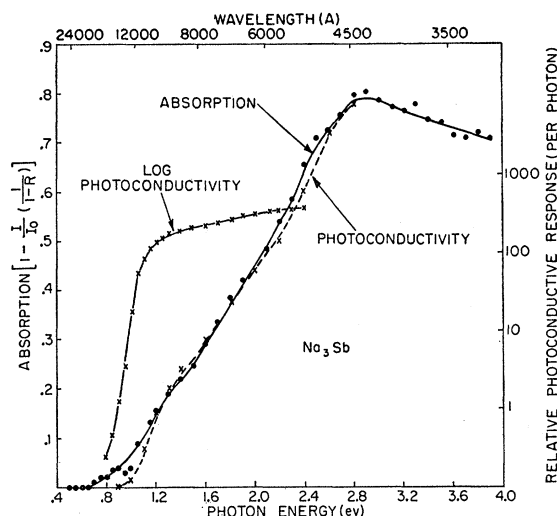


FIG. 5. Absorption and photoconductivity of Na_3Sb . A band gap of 1.1 eV is obtained from these data.

2.4 eV with peaks at 2.6 and possibly 3.8 eV and a minimum at about 3.1 eV (Fig. 4). This structure very definitely seems to be real and not associated with any interference effects. The multi-alkali material had the slowest rate of rise of any of the materials, reaching its peak value only at about 3.2 eV (Fig. 2). By taking absorption curves of samples of different thicknesses, it was ascertained that these features were characteristic of the materials and not due to the thickness of the particular samples.

IV. PHOTOEMISSION

A. A Model for Photoemission from Semiconductors

Photoemission can be thought of as a three-step process consisting of (1) photoexcitation of the electrons, (2) the motion of the electrons through the crystal, and

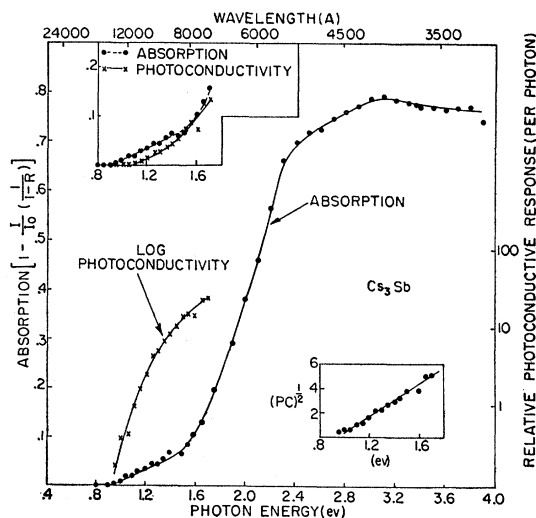


FIG. 6. Absorption and photoconductivity of Cs_3Sb . A plot of the square root of photoconductivity vs $h\nu$ is given in the insert.

(3) the escape of the electrons over the surface barrier (electron affinity) into the vacuum. Here the photoemission due to fundamental absorption, i.e., transitions from valence to conduction band, will be considered. The absorption process will be discussed with the help of a diagram of energy versus the virtual crystal momentum k (Fig. 7). The bands have been assumed to be parabolic with extrema at the same k value; however, this part of the discussion would not be changed by any more generalized band structure. E_G is the band gap energy and E_A is the electron affinity, i.e., the energy

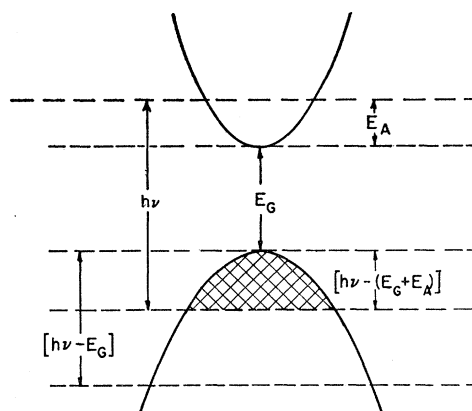


FIG. 7. A plot of energy vs k . E_G is the band gap energy and E_A is the value of the electron affinity. For convenience, the valence band energy will be measured as increasing downward from the top of the band. For the arbitrary value of photon energy, $h\nu$, given in the figure, transitions from valence band states lying between the top of the band and an energy level of $[h\nu - (E_G + E_A)]$ will result in electrons excited above the vacuum level (corresponding to an absorption coefficient α_p). Absorption is also possible from valence band states lying between $[h\nu - (E_G + E_A)]$ and $(h\nu - E_G)$. However, this will result in excitation to conduction band states below the vacuum level (corresponding to the absorption coefficient α_c) and cannot give rise to photoemission.

difference between the bottom of the conduction band and the vacuum level. It is convenient to subdivide the absorption into two types and to define absorption coefficients for each. α_c will represent the absorption coefficient for all the transitions in which the final state lies below the vacuum level; whereas α_p will represent the transitions to levels above the vacuum level. Thus, only the absorption associated with α_p can possibly give rise to photoelectric emission. The total absorption coefficient, α_T , will be the sum of α_p and α_c .

The remaining two parts of the photoelectric process can be lumped together and considered as the probability of escape, $P(x, h\nu)$, a function of both the distance, x , from the surface at which the electron is produced and the photon energy, $h\nu$. The latter dependence is due to the fact that kinetic energies with which the electrons are excited will be a function of $h\nu$. Thus the general expression for the photoemission current will be

$$i(h\nu)d(h\nu) = \int_0^{\infty} \alpha_p(h\nu)I(x, h\nu)P(x, h\nu)dx d(h\nu). \quad (1)$$

Here, $i(h\nu)$ is the photoemission current due to the light of photon energy $h\nu$, $d(h\nu)$ is the band pass of the monochromator used, $I(x, h\nu)$ is the intensity of the light at a depth x from the surface, and the integration is over x . The sample thickness has been assumed to be sufficiently large so that the upper limit of the integral can be taken as infinity. $I(x, h\nu)$ is given by

$$I(x, h\nu) = I_0(h\nu)e^{-\alpha_T x}, \quad (2)$$

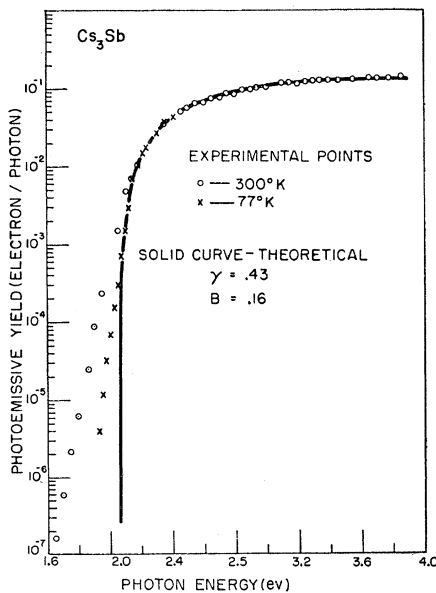


FIG. 8. Photoemission from Cs_3Sb . The points are experimental and the solid curve is theoretical. As with the other materials which showed p -type behavior, cooling decreases the photoemission in the threshold region. The room temperature and liquid N_2 temperature points have been fitted vertically. An $E_G + E_A$ value of 2.05 eV is obtained.

where $I_0(h\nu)$ is the incident photon flux. The photoemission yield, $Y(h\nu)$, will be $i(h\nu)/I_0(h\nu)$. In order to integrate Eq. (1), a function of the form

$$P(x, h\nu) = G(h\nu)e^{-\beta x} \quad (3)$$

has been assumed, where $G(h\nu)$ is an, as yet, undefined function of $h\nu$ and β is a constant. This form seems to be the simplest which will fit the experimental data. The exponential dependence is such as might be expected for diffusion with absorption and has been found to be applicable in secondary emission.²⁰ Under these assumptions, we may integrate Eq. (1) to obtain the photoemission yield:

$$Y(h\nu) = \left(\frac{\alpha_p(h\nu)}{\alpha_T(h\nu) + \beta} \right) G(h\nu). \quad (4)$$

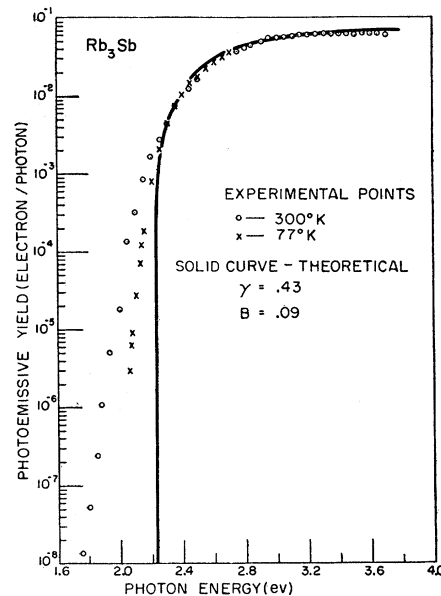


FIG. 9. Photoemission from Rb_3Sb . The points are experimental and the solid curve is theoretical. Room temperature and liquid N_2 temperature points have been fitted vertically. An $E_G + E_A$ value of 2.05 eV is obtained.

It should be noted that if the escape probability were unity, the yield would be determined by α_p/α_T . In any case, where $\alpha_T(h\nu)$ is of the same order or larger than β , the ratio $\alpha_p(h\nu)/\alpha_T(h\nu)$ will be important in determining $Y(h\nu)$; that is, if the light is absorbed within a distance from the surface comparable to $1/\beta$, the reduction in yield due to the electrons excited into states below the vacuum level will be very important. From Burton's work,⁴ it appears that α_T and β are comparable in Cs_3Sb . Thus these considerations are of importance for Cs_3Sb and probably for the other materials studied here. A rather rough measure of the value of $\alpha_c(h\nu)/\alpha_T(h\nu)$ in the spectral region several

²⁰ A. J. Dekker, *Solid State Physics* (Prentice-Hall, Inc., Englewood Cliffs, New Jersey, 1957), Chap. 17.

electron volts removed from the threshold where the yield becomes relatively constant may be obtained from the ratio of the absorption coefficient at the threshold of photoemission to the maximum value of the absorption coefficient in the blue or ultraviolet.

B. Application of the Model to the Alkali-Antimonide Compounds

In order to make a specific calculation, it is necessary to consider the absorption coefficients $\alpha_p(h\nu)$ and $\alpha_c(h\nu)$. Recognizing the fact that near the threshold of emission $\alpha_p(h\nu)$ will be varying with $h\nu$ much faster than $\alpha_T(h\nu)$, it can be seen from Eq. (4) that the photon energy dependence of $Y(h\nu)$ will be determined by that of $\alpha_p(h\nu)G(h\nu)$. As will be shown later, it was

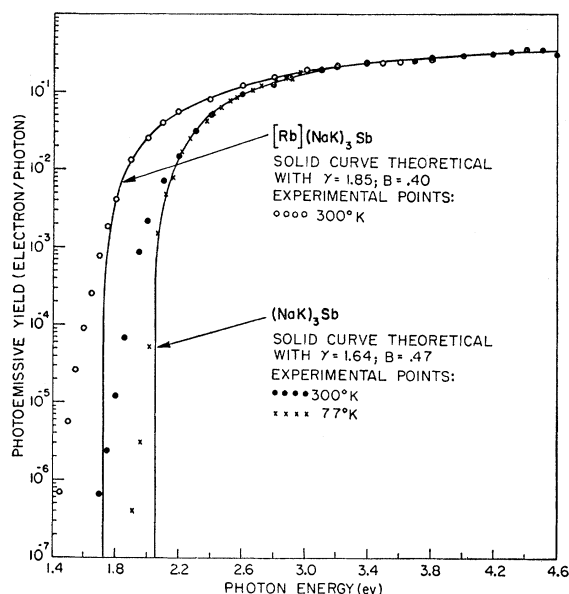


FIG. 10. Photoemission from $(\text{NaK})_3\text{Sb}$ and $[\text{Rb}](\text{NaK})_3\text{Sb}$. The points are experimental and the solid curve is theoretical. Room temperature and liquid N_2 temperatures points have been fitted vertically. $E_G + E_A$ values of 2.0 and 1.7 eV are obtained for $(\text{NaK})_3\text{Sb}$ and $[\text{Rb}](\text{NaK})_3\text{Sb}$, respectively.

found that $G(h\nu)$ could usually be treated as a constant. Thus the photoelectric yield near the threshold should be proportional to $\alpha_p(h\nu)$. Experimentally, the yield was found to vary as $[h\nu - (E_G - E_A)]^{3/2}$ in this region, indicating such a dependence of $\alpha_p(h\nu)$. With a parabolic valence band, this would indicate an unallowed direct transition²¹ or any type of transition which is just proportional to the total number of states in the valence band from which photoelectrons may be obtained.²² Thus α_p has the form

$$\alpha_p = C[h\nu - (E_A + E_G)]^{3/2}, \quad (5)$$

²¹ Bardeen, Blatt, and Hall, in *Proceedings of the Conference on Photoconductivity, Atlantic City, 1954*, edited by R. G. Breckenridge, et al. (John Wiley and Sons, Inc., New York, 1956), pp. 148-150.

²² Note that for Cs_3Sb $\alpha_T(h\nu)$ goes as $(h\nu - E_G)^{3/2}$. See references 6 and 19.

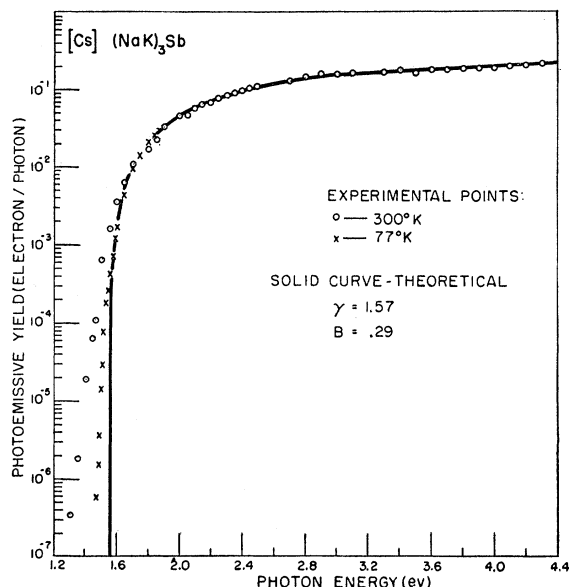


FIG. 11. Photoemission from $[\text{Cs}](\text{NaK})_3\text{Sb}$. The points are experimental and the solid curve is theoretical. Room temperature and liquid N_2 temperature points have been fitted vertically. An $E_G + E_A$ value of 1.55 eV is obtained.

where C is a constant. As will be seen later, the electron affinities found here are larger than a few tenths of an electron volt; thus, it can be shown that the final results are not significantly changed by taking $\alpha_c(h\nu)$ to be a constant rather than proportional to $(h\nu - E_G)^{3/2}$. Using this approximation and putting (5) into (4), we obtain

$$Y(h\nu) = \frac{[h\nu - (E_G + E_A)]^{3/2} G(h\nu)}{[h\nu - (E_G + E_A)]^{3/2} + \gamma}, \quad (6)$$

where

$$\gamma = (\alpha_c + \beta)/C \quad (7)$$

is a parameter determined by fitting to the experimental data.

C. Experimental Results

1. Cs_3Sb , Rb_3Sb , and the Multi-Alkali Photoemitters

It was found that Cs_3Sb , Rb_3Sb , and three multi-alkali materials could be fitted by the model proposed above. In all cases, photoemissive curves were obtained from the thin samples used for the absorption and photoconductive studies and also from samples of a thickness greater than the optical absorption length of the material in order to justify the integration from zero to infinity in equating (1). It was found that most multi-alkali, Cs_3Sb , and Rb_3Sb data could be fitted by this model with $G(h\nu)$ taken as a constant, B , independent of $h\nu$. Such data are given in Figs. 8 through 11. The values taken for B and γ to fit the data are indicated on each plot.

The results for Cs_3Sb are shown in Fig. 8. The theoretical curve could be fitted to the experimental

data in the region of $h\nu$ greater than 2.0 eV. From this fit, a value of 2.05 eV is obtained for $E_G + E_A$. In the lower energy region, the experimental data diverge from the theoretical curve as would be expected if the yield in this region were due to photoexcitation from impurity states. Since there is evidence that these materials are p type, this photoemission would seem to come from filled acceptors. Cooling the material to liquid N_2 temperature should decrease such an impurity photoemission. Figure 8 shows that such an effect was, in fact, observed.²³ Thus, the photoemission in the threshold region seems to come from acceptor-type impurity states. A sharpening of the slope of the yield curve on cooling is also evident here as in the case of the other materials. This effect will be discussed later.

The data obtained from Rb_3Sb are shown in Fig. 9. The shape of the curve is similar to that for Cs_3Sb , the principal difference being that in the threshold region, the change of slope of the yield curve on cooling was much less than for Cs_3Sb . A value for $E_G + E_A$ of 2.2 eV is obtained from the fit.

Figures 10 and 11 show the results obtained from the multi-alkali cathodes. Again, the theory may be fitted to the data in the range of high yields. The change of yield with temperature in the threshold region is as would be expected for acceptor states. The values of $E_G + E_A$ are 2.0 eV for $(NaK)_3Sb$, 1.55 eV for $[Cs](NaK)_3Sb$, and 1.7 eV for $[Rb](NaK)_3Sb$. The $[Rb](NaK)_3Sb$ was not studied extensively and no low-temperature data were taken from this type of surface. As mentioned before, within experimental error, the absorption and photoconductivity of the layers were not affected by the addition of the third alkali metal; the effect of the addition of Cs or Rb was to reduce the electron affinity. This reduction is about 0.45 eV for Cs and 0.3 eV for Rb.

The curves shown here are representative of the majority taken for these surfaces. However, a minority, about 10% for the single alkalis and 30% for the multi-alkali materials, could not be easily fitted if the assumption of constant $G(h\nu)$ was made. Instead, it seemed necessary to assume that $G(h\nu)$ was a function which increased rather slowly with $h\nu$ [e.g., $G(h\nu)$ might increase by a factor of about 2 over a $h\nu$ range of about 1.5 eV]. This variation of the escape probability between samples may be caused by such parameters as the number and types of defects present, the bending of the bands at the glass and vacuum interfaces of the samples, and/or crystallite size. That the multi-alkali surfaces vary from the simple theory much more often than the single alkali would seem to reflect their greater complexity and thus a stronger probability for variation in these parameters.

It is also of interest to consider the impurity photo-

²³ It was impossible to measure the absolute yield of the cooled photoemitters. Thus, the yield curves taken at liquid N_2 temperature have been fitted vertically to the room temperature curves in the region of fundamental photoemission.

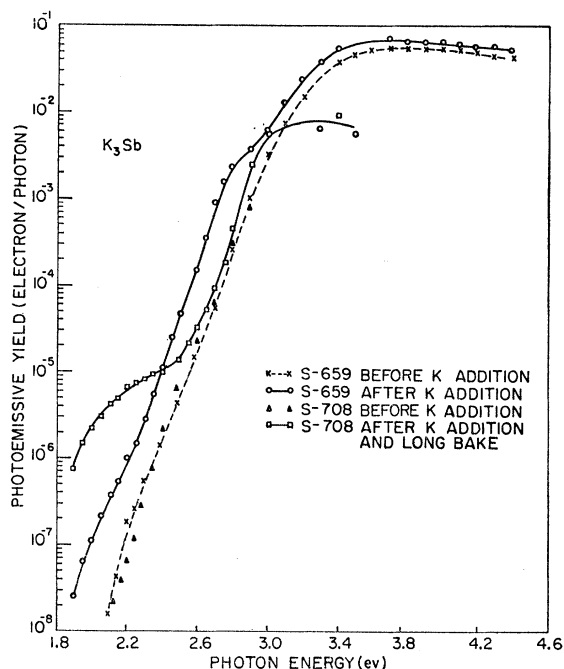


FIG. 12. Photoemission from K_3Sb . These data could not be fitted by theoretical curves. Impurity photoemission centered at about 2.1 eV and perhaps 2.8 eV is present. The value for $E_G + E_A$ probably lies between 2.2 and 2.9 eV.

emission. The acceptor states giving rise to this emission may be bulk states or may be associated with the surface. The lack of structure in the low-energy region of the photoemissive response curve indicates a lack of well-defined levels and, thus, a distribution of impurity states increasing in something like an exponential manner with energy above the top of the valence band. If such were the case, the slope of the yield curve should increase by about a factor of 4 on cooling from 300° to $77^\circ K$. Such an increase was found for $[Cs](NaK)_3Sb$. The change in slope is less for the other materials. This would be expected if the low-temperature response were due to compensated rather than thermally filled acceptors.

The deduction that the threshold photoemission is due to acceptors agrees, in general, with the findings of Borzyak,⁹ Sakata,¹⁰ and Sommer.¹¹ The only question arises in the case of Rb_3Sb in which Sommer did not find definite evidence for p -type conduction from resistance measurements.

A density of impurity levels of 10^{19} to $10^{20}/cm^3$ would have to be assumed to agree with the magnitude of the impurity photoeffect. This is in agreement with the values estimated for Cs_3Sb from conductivity and Hall measurements by Sakata.^{10,24} The difference measured here between the threshold for fundamental response and the threshold for impurity response (about 0.45 eV) for Cs_3Sb lies in the range of activation energies

²⁴ T. Sakata, J. Phys. Soc. Japan 8, 793 (1953).

0.2–0.7 eV obtained from conductivity *vs* temperature curves measured by a number of workers.^{25–29} The distribution of impurity states indicated by our data may help to explain the range of activation energies found by these workers.

2. Photoemission from Na_3Sb and K_3Sb

Typical spectral response curves obtained from Na_3Sb and K_3Sb are shown in Figs. 12 and 13. These could not be fitted to the theoretical model. The response in the threshold region was found to vary strongly from sample to sample. It is believed that this variation can be correlated with the presence of excess alkali metal in the lattice. Figure 12 indicates clearly the increase in threshold yield for two K_3Sb layers with the addition of *K*. The relatively low peak efficiency of sample S-708 after *K* addition is due to the fact that it was irradiated from the glass substrate and most of the light was absorbed too deeply in the material to give rise to photoemission. It was impossible to follow the photoemission of S-708 to the spectral range in which higher yield occurs before *K* addition because of the difficulty of drawing saturation current from the highly resistive layer. From these data, there is evidence of an impurity photoemission band centered at about 2.1 eV which is induced by *K* addition. S-659 also showed evidence of a second impurity band due to *K* addition at about 2.8 eV.

As can be seen in Fig. 13, two general features appear in all Na_3Sb curves; the break at about 3.4 eV which probably indicates the appearance of impurity photoemission and the plateau region beginning at about 4.4 eV. As shown in Fig. 13, it was found that the yield in the region below 3.4 eV can be increased by Na addition. The break between impurity and intrinsic photoemission also sharpened on cooling and the yield in the impurity region increased as would be expected if electrons were being condensed into the impurity levels. The same behavior on cooling was observed in K_3Sb . Since it is impossible to fit the theoretical curves to these data, no criteria exists by which exact values of the electron affinities may be obtained. However, it is possible to set reasonable upper and lower limits of the electron affinity. Since photoemission at photon energies less than the electron affinity would not be expected, the upper limit is set by the minimum value of $h\nu$ for which photoemission is detectable. The lower limit will be assumed to be given by

$$E_A > h\nu_B - 0.3 \text{ eV}, \quad (8)$$

where $h\nu_B$ is the photon energy at which the intrinsic

²⁵ W. J. Harper and W. J. Choyke, *J. Appl. Phys.* **27**, 1358 (1956).

²⁶ N. Schaetti and W. Baumgartner, *Le Vide* **6**, 1041 (1951); *Helv. Phys. Acta* **24**, 614 (1951).

²⁷ R. Suhrman and C. Kangro, *Naturwissenschaften* **40**, 137 (1953).

²⁸ T. Sakata, *J. Phys. Soc. Japan* **8**, 125, 723, 793 (1953).

²⁹ T. Sakata and S. Munesue, *J. Phys. Soc. Japan* **9**, 141 (1954).

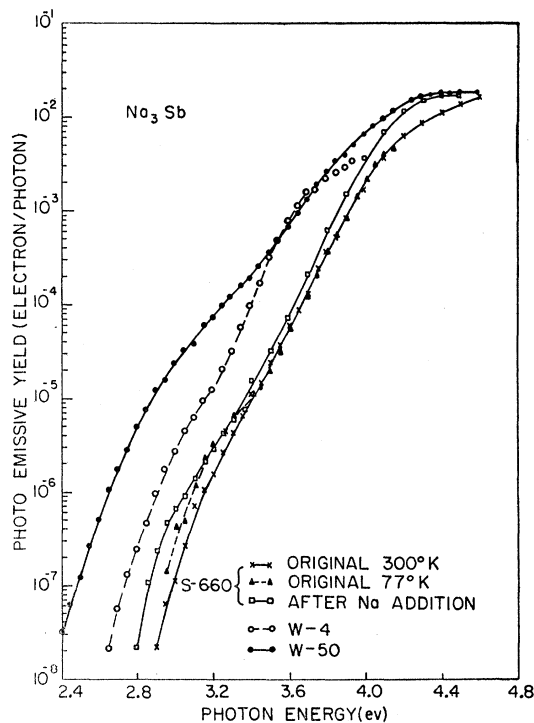


FIG. 13. Photoemission from Na_3Sb . These data could not be fitted by theoretical curves. The photoemission below about 3.4 eV is probably due to impurities. The value for $E_G + E_A$ probably lies between 3.2 and 3.5 eV.

photoemission breaks away from the impurity photoemission. This is 3.5 eV in the case of Na_3Sb and 2.5 eV for K_3Sb . By this means, the electron affinity of K_3Sb is estimated to lie between 1.8 and 1.1 eV and that for Na_3Sb between 2.4 and 2.0 eV.

The inability to fit the theoretical equations to Na_3Sb and K_3Sb may be due to the fact that the fundamental photoemission is obscured by the impurity emission. The difficulty is also increased by the high photon energy threshold of these materials. This limits the range over which the fundamental photoemission may be studied. However, the salient difference between these response curves and those that do fit the theoretical curves is the rather slow rate of rise of yield in the intrinsic region. For example, it takes a photon energy range over 1.0 eV for the K_3Sb response to rise from 10^{-7} to 10^{-2} electron/photon; whereas, the materials which fit the model rise by this amount in less than 0.5 eV. This difference might be due to a strong $h\nu$ dependence on escape probability or a turning up of the bands at the vacuum interface in the case of K_3Sb and Na_3Sb or to other causes.

V. SUMMARY OF RESULTS

The values for the band gap E_G and the electron affinity E_A (obtained by subtracting E_G from $E_G + E_A$) are tabulated in Table I. The conductivity type as

TABLE I. Values for band gap (E_G) and electron affinity (E_A). Conductivity type was determined from photoemission measurements. Peak quantum efficiency was obtained from measurements on a number of samples.

Material	Type	E_G (ev)	E_A (ev)	Peak quantum efficiency measured
Na ₃ Sb	<i>n</i>	1.1	2.0-2.4	0.02
K ₃ Sb	<i>n</i>	1.1	1.1-1.8	0.07
Rb ₃ Sb	<i>p</i>	1.0	1.2	0.10
Cs ₃ Sb	<i>p</i>	1.6	0.45	0.25
(NaK) ₃ Sb	<i>p</i>	1.0	1.0	0.30
[Rb](NaK) ₃ Sb	not measured	1.0	0.70	...
[Cs](NaK) ₃ Sb	<i>p</i>	1.0	0.55	0.40

indicated by the photoemission data is also listed. Except for Rb₃Sb, the conductivity type found here is identical with that found by Sommer.¹¹ The peak quantum efficiency listed is the highest value obtained from measurements on a number of samples. No value is given for [Rb](NaK)₃Sb since only a few tubes of this type were measured.

VI. DISCUSSION

The band gaps of the alkali antimonides do not appear to vary appreciably with the alkali constituent, except in the case of Cs₃Sb. Since Cs₃Sb has a "pseudo-body-centered cubic"²² structure whereas the other single alkali materials have a Na₃As-type hexagonal structure,^{2,30} this difference may be related to crystal structure. (The structure of the multi-alkali antimonides is not known at present.) The lack of variation of band gap with alkali constituent for the materials having the Na₃As structure is similar to the effect found in the alkali halides where the band gap is little affected by a change in the alkali constituent. In contrast to the small differences in the band gaps of Na₃Sb, K₃Sb, and Rb₃Sb, the electron affinities of these materials decrease quite markedly with increasing atomic number of the alkali constituent. The values of the peak quantum efficiency vary in the same way.

It is interesting to note the considerable difference between the electron affinities of Na₃Sb and K₃Sb and that of (NaK)₃Sb. This is in contrast to the small

³⁰ A. L. Solomon (private communication).

difference in the band gap energies. Thus, the increase in photoelectric efficiency of the "multi-alkali" cathodes over that of K₃Sb or Na₃Sb seems to be mainly due to a reduction in electron affinity and may be caused by the formation of a favorable dipole layer at the surface, the change in the conductivity type of the material as discussed below, or a combination of these. The reduction of the electron affinity of (NaK)₃Sb by addition of Cs and Rb is also quite striking and would seem to be due solely to an increasingly favorable dipole layer at the surface.

Cs₃Sb and (NaK)₃Sb have comparable peak quantum efficiencies although their electron affinities are quite different. This is probably related to the fact that the ratios of the absorption coefficient at the threshold of photoemission to the maximum absorption coefficient are about equal for these two materials [see Sec. IV (A) and Figs. 2 and 6]. The increased peak yield of [Cs](NaK)₃Sb over (NaK)₃Sb can probably be related to a decrease in this ratio (i.e., a decrease in the fraction of the excited electrons which go into states below the vacuum level).

The data show that the most efficient emitters are those with *p*-type electrical properties. If one considers the effect of surface states, it is easy to see that for the *n*-type materials the bands will have a tendency to turn upward at the surface; whereas, for *p*-type materials, the bands will tend to turn downward. Such behavior will be reflected in an effective raising or lowering of the electron affinity. In particular, the fact that the electron affinity of (NaK)₃Sb is less than that of Na₃Sb or K₃Sb may be partially due to the fact that the former is *p* type and the latter *n* type.

ACKNOWLEDGMENTS

The author wishes to thank A. H. Sommer for the preparation of the materials studied and for many helpful discussions and H. B. DeVore who designed and built the equipment associated with the monochromator. He also wishes to thank G. A. Morton, A. Rose, E. G. Ramberg, R. M. Matheson, and R. H. Parmenter for many helpful discussions and G. O. Fowler for aid in the reduction of data, and to express his appreciation to J. A. Burton and W. J. Choyke for unpublished information.